Computers in Biology and Medicine 108 (2019) 101–110

Contents lists available at ScienceDirect

Computers in Biology and Medicine

journal homepage: www.elsevier.com/locate/compbiomed

Symmetrical cruciate-retaining versus medial pivot prostheses: The effect of intercondylar sagittal conformity on knee kinematics and contact mechanics

Liming Shu[a,*], Ko Yamamoto[b], Shin Kai[c], Junichi Inagaki[c], Naohiko Sugita[a]

[a] Department of Mechanical Engineering, School of Engineering, The University of Tokyo, 7-3-1 Hongo, Bunkyo-ku, Tokyo, 113-8656, Japan
[b] Department of Mechano-Informatics, Graduate School of Information Science and Technology, The University of Tokyo, 7-3-1 Hongo, Bunkyo-ku, Tokyo, 113-8656, Japan
[c] Robert Reid Inc, 4-22-2 Koishikawa, Bunkyo-ku, Tokyo, 112-0002, Japan

ARTICLE INFO

Keywords:
Total knee arthroplasty
Medial pivot
Kinematics
Contact mechanics
Finite element

ABSTRACT

Background: A total knee arthroplasty should restore the mechanical function of the knee and enable patients to perform desired daily activities. The joint kinematics and contact mechanics performance are important determinants of the success of total knee arthroplasty devices. The purpose of this study was to determine the effect of intercondylar sagittal conformity on kinematics and contact mechanics.

Methods: An explicit dynamic finite element method was used to investigate the differences in the performances of constrained cruciate-retaining (CR), unconstrained CR, and medial pivot designs during gait, squatting, descending stairs, and climbing stairs. The predicted kinematic results were verified through an *in vitro* experiment during the gait cycle.

Results: The results confirmed that the medial pivot design improved the kinematic behavior with no paradoxical anterior motion, which was found in the unconstrained prosthesis during the four activities. However, a small femoral internal rotation was found during gait (3.9°), descending stairs (2.2°), and climbing stairs (3.6°), which may produce anterolateral pain. An enlarged contact area and a lower peak contact pressure were observed on the medial side of the medial pivot prosthesis. Conversely, on the lateral side of the medial pivot prosthesis, the contact area and peak contact pressure were equal to those of the unconstrained prosthesis, which could potentially result in wear.

Conclusion: In summary, although the medial pivot prosthesis may provide qualitatively similar kinematics as the average measurements of tibiofemoral motion, further *in vivo* analysis and long-term studies on the femoral internal rotation and high contact pressure on the lateral side are still required.

1. Introduction

The objective of total knee arthroplasty (TKA) is to restore the mechanical function of the knee and enable patients to perform desired daily activities. To mimic the biomechanics of a normal knee joint, a wide range of prostheses have been designed and evaluated since the 1950s [1]. However, several current symmetrical cruciate-retaining (CR) TKA designs cannot provide normal knee kinematics and some are prone to paradoxical anterior sliding of the femur on the tibia during daily activities, which would have a negative impact on a patient's joint [2–4]. Furthermore, the large anterior translation of the femoral component on the surface of the tibial polyethylene (TP) component would accelerate the wear of the TP component and reduce the prosthesis service life [5]. The non-anatomic and symmetric geometric interface of contemporary implants are one of the reasons that the kinematics of the lower limb are altered in TKA patients. These implants exhibit crossed-four-bar linkage kinematics that conflict with the natural movement of the femur relative to the tibia [6]. Recent studies on normal knee kinematics have illustrated that a statistically relative larger translation is found on the lateral side compared to that on medial side, which is known as medial pivot motion [7–11].

In recent years, a new design of the medial pivot knee prosthesis (MPKP), which is characterized by a different intercondylar sagittal conformity between the lateral and medial side of the knee, has received considerable attention for use in TKA [12–15]. This design was developed to achieve medial-centered rotation as exhibited by a normal knee and to reduce the wear of the TP component by creating a near constant femoral component radius. As reported by Fen et al. [16], the MPKP provided a statistical improvement in the postoperative range of motion, objective knee society score, pain scale, and functional score.

* Corresponding author.
E-mail address: l.shu@mfg.t.u-tokyo.ac.jp (L. Shu).

https://doi.org/10.1016/j.compbiomed.2019.03.005
Received 30 October 2018; Received in revised form 6 March 2019; Accepted 7 March 2019

Karachalios et al. [17] also obtained satisfactory mid-term clinical results for patients with a MPKP. However, there are controversial results regarding the clinical outcome of MPKPs. Kim et al. [18,19] reported a lower knee score, smaller range of knee motion, and lower patient satisfaction of an MPKP group, compared with those of a press fit condylar (PFC) mobile-bearing prosthesis group. Papagiannis et al. [20] stated that no kinematics and kinetic advantages were observed during gait for the MPKP compared to the rotating platform prosthesis. In addition, with respect to the success of TKA devices, both the kinematic analysis and contact mechanics should be considered as important factors that influence the TP component wear [21–23]. However, there are few studies regarding the contact mechanics of the MPKP [24].

As it is difficult and costly to measure kinematics and contact mechanics experimentally *in vivo* and *in vitro*, a computational model has been proposed as an efficient method for performing an evaluation of the TKA design under various dynamic loading conditions. Varadarajan et al. [25] used the rigid dynamics method in the commercial LifeMOD KneeSIM software to analyze the kinematic differences among various prostheses. However, it is difficult to simultaneously predict accurate kinematics and contact mechanics. An explicit dynamic finite element method (FEM) has been employed in order to develop dynamic tibiofemoral models that have the capability of simultaneously determining the joint kinematics and contact mechanics [26–30]. However, these studies have focused on the gait cycle without evaluating other daily activities such as climbing stairs and deep squatting.

In this study, a comparison of the symmetrical CR and MPKP designs was performed with respect to their kinematics and contact mechanics using an explicit dynamic FEM for simulating daily activities, such as gait, deep squatting, descending stairs, and climbing stairs, to understand the effect of the intercondylar sagittal conformity. The simulated kinematic results for the gait cycle were also verified using *in vitro* experimental data.

2. Material and methods

2.1. Finite element model

Explicit FE models of three tibiofemoral knee prostheses were developed using the commercial FE software Abaqus (Dassault Systems Simulia Corp., Johnston, USA) to simulate daily activities on the Stanmore knee simulator [31]. To study the effect of intercondylar sagittal conformity on knee joint kinematics and contact mechanics, three implants with different conformities were chosen in this study. The conformity of the model was defined as the difference between the corresponding femoral and tibial curvature in the sagittal plane [32]. The selected commercial MPKP design (Fig. 1 (a)) (Adler Ortho S.R.L, Cormano, Italy) has an asymmetrical TP, whose conformities on the medial and lateral sides were approximately 0.99 and 0.3, respectively. As a comparison, two CR knee prostheses were selected including a posterior cruciate-retaining (CPCR) design (Fig. 1 (b)) (Adler Ortho S.R.L, Cormano, Italy) with a high conformity (0.99) and unconstrained posterior cruciate-retaining (UPCR) design (Fig. 1 (c)) (DePuy International, Leeds, UK) with a low conformity (0.3). The sagittal curve on the medial side of the TP of the MPKP was similar to that of the CPCR, while that on the lateral side was similar to that of the UPCR. In addition, to eliminate the influence of the mobile bearings, the rotation between the TP component and tibial tray was fixed in the simulation and experiments. A detailed description of the three prostheses are shown in Table .1. It is noteworthy that the sagittal curve of the UPCR is multi-radius, which means that the sagittal conformity changes with the flexion angle. We only focused on the analysis of the difference in the sagittal conformities of the three designs, instead of the effects of each specific structural parameter of the femoral and tibial components.

The femoral component and tibial tray were modeled as rigid bodies owing to their Young's modulus, which is significantly higher than that of the TP component, and were meshed using a C3D4 tetrahedron with a 1.5-mm element length. The femoral component of the UPCR comprised 55,552 elements, while that of the MPKP and CPCR comprised 75,327 elements. The tibial tray of the UPCR comprised 64,493 elements, while that of the MPKP and CPCR comprised 24,395 elements. The TP component was modeled as a non-linear elastic–plastic material (UHMWPE) with a modulus of elasticity of 463 MPa and a Poisson's ratio of 0.46 using the experimental stress–strain data [33]. It was meshed using 10-node modified quadratic tetrahedral elements (C3D10 M) with a 1.3-mm element length based on the convergence study. The TP component of the CPCR, UPCR, and MPKP comprised 34,920, 51,330, and 40,712 elements, respectively. The coefficients of friction for the contact surfaces between the femoral and TP components were set to 0.04 in accordance with the artificial joints and experimental pin-on-disk tests, as well as previous computational models [34,35]. A nonlinear surface-to-surface penalty property with contact geometry corrections was assigned to the contact surfaces.

2.2. Boundary conditions and loading

The Stanmore knee simulator is a well-established force-controlled knee simulator in which *in vivo* environments of the knee joint are replicated by applying the appropriate forces and moments to the femoral and tibial components [32,36]. The boundary conditions applied to the model were based on the Stanmore knee simulator, as shown in Fig. 2. The femoral component was allowed to rotate along the transverse axis to simulate flexion–extension (F–E) rotation. The degrees of freedom of the inferior–superior (I–S) translation and valgus–varus (V–V) rotation on the femoral component were unconstrained. The TP component was

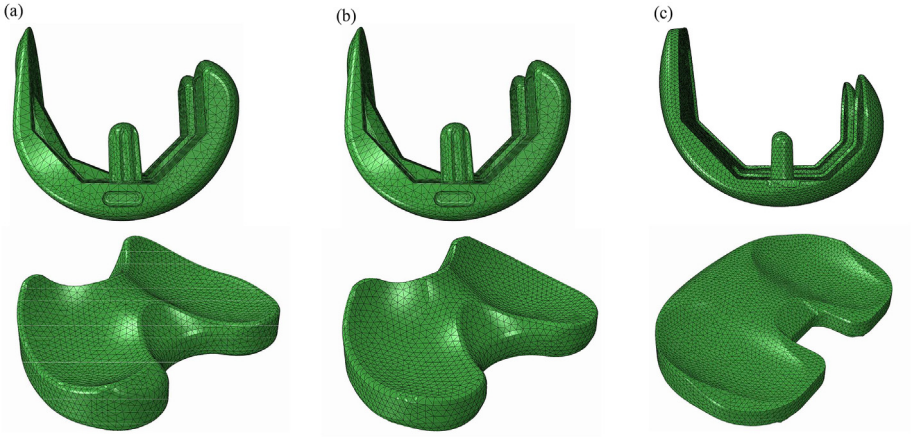

Fig. 1. FE meshed model. (a) Femoral and TP components of the MPKP, (b) femoral and TP components of the CPCR, (c) femoral and TP components of the UPCR.

Table 1
Description of the knee prostheses used in this study.

Prosthesis	Femoral Component	TP component	
		Medial side	Lateral side
CPCR	Single-radius	High conformity (0.99)	High conformity (0.99)
UPCR	Multi-radius	Low conformity (0.30)	Low conformity (0.30)
MPKP	Single-radius	High conformity (0.99)	Low conformity (0.30)

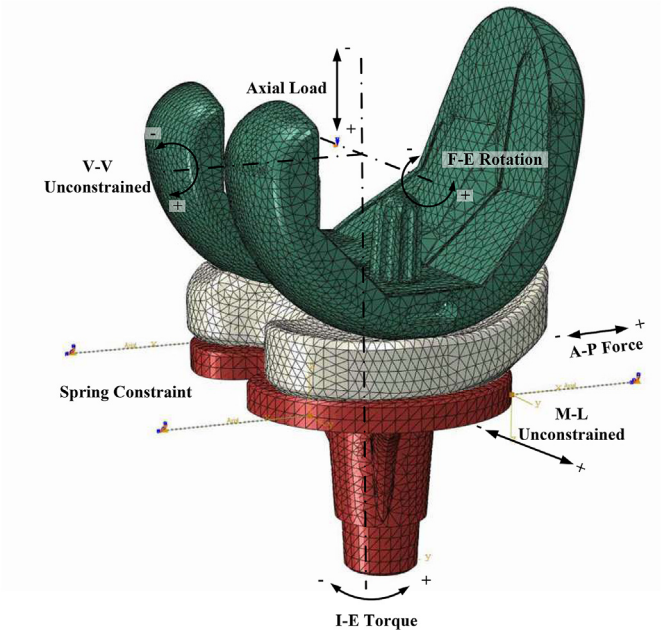

Fig. 2. FE model of the TKA model for force-control loading conditions (Note: the positive A-P force acts in the anterior directions; the positive axial force component is acts distally in the inferior direction along with the implant shaft; and the positive I-E torque turns clockwise around the outer rotation of the tibia).

allowed to perform unconstrained motion in the medial–lateral (M–L) direction. To simulate the ligaments and soft tissue constraints around a knee joint, a set of nonlinear springs was included in the TKA model [37]. The detailed resistance was set and simplified based on the physiological restraint of an intact knee [38]. The translation resistance was set to 9.3 N/mm based on ISO 14,243–1:2009. In addition, the resistance was assumed zero for the TKA prosthesis within 2.5 mm in either direction of the reference point to include the small restraint stiffness of soft tissue around the knee joint. The rotation resistance was 0.36 Nm/°. The rotation resistance was also zero for the TKA prosthesis within ± 6° from the reference position. The axial load axis was shifted by 7% of the TP component width in the medial direction to simulate the natural various loadings of the knee joint.

To analyze the kinematics and contact mechanics of the three designs, the loading conditions for daily activities including gait, squatting, descending stairs, and climbing stairs were applied in the model, as shown in Fig. 3. The gait data were obtained based on ISO 14,243–1:2009. The loading inputs for squatting, descending stairs, and climbing stairs were measured *in vivo* and averaged for eight subjects with instrumented knee implants [39]. The F–E rotation was measured using a motion capture system and calculated using inverse kinematics with a high accuracy [40–42].

2.3. Experimental validation

The gait cycle was selected as the sample activity for evaluating the accuracy of the simulation results. The same size of prostheses that were modeled in the simulation were used in the experimental validation. The simulated kinematic results were verified by comparing the experimental results using the Stanmore knee simulator. The boundary condition of gait cycle was based on the ISO standard (ISO 14,243–1:2009), as shown in Fig. 3.

3. Results

3.1. Model validation

All of the predicted results were in good agreement with the experimental results, in terms of the trend and magnitude, as shown in Fig. 4. The A–P translation and I–E rotation of the UPCR are also well consistent with the results from previous studies [43,44]. However, during 65% of the gait cycle, the predicted translation and rotation did not agree well with the experimental data, possibly owing to the neglected mass and inertia of the simulator fixtures. In this study, the validation of the model was only performed on the gait cycle for three prostheses due to cost and time issues. However, good agreement between the simulated and experimental results was obtained during the gait cycle, which supports the assumption that the finite element simulator mimics the Stanmore knee simulator with a high accuracy.

3.2. Kinematic difference

During the gait cycle, the femoral component of the CPCR was approximately fixed on the TP component, and the maximum translation (1.2 mm) of the femoral medial condyle was in the anterior direction, as shown in Fig. 5 (a). The UPCR exhibited a more flexible character than that of the CPCR (Fig. 5 (b)). A large anterior translation (6.4 mm) and an external rotation (−2.6°) were observed during the loading response phase. The maximum posterior translation (−1.7 mm) was obtained in the swing phase, and an internal rotation (9.1°) was obtained in the pre-swing phase. Because of the high conformity of the medial side of the MPKP, which was the same as that of the CPCR, the MPKP exhibited a lower femorotibial translation on the medial side than that of the UPCR (case Fig. 5 (c)). An external rotation (−2.8°) and an internal rotation (3.9°) were observed during the load response and pre-swing phases, respectively.

During the squatting cycle, the CPCR, UPCR, and MPKP all showed external rotations (−3.8°, −8.4°, and −11.3°, respectively) and posterior translations (−1.4 mm, −5.7 mm, and −0.9 mm, respectively) during the flexion phase, as shown in Fig. 6. However, only the UPCR, case exhibited an anterior translation (4.7 mm) during the extension phase.

Various performances during the descending stairs cycle for the three prostheses are shown in Fig. 7. Hinge-joint kinematics were observed in the CPCR, which was similar to the movements during gait and squatting (Fig. 7 (a)). For the UPCR, an anterior translation (2.2 mm) and external rotation (−1.4°) of the femoral medial condyle were observed when the heel contacted the stairs, while a posterior translation (−1.9 mm) and an external rotation (−10.1°) were observed during the swing phase. A small internal rotation (0.5°) was observed for approximately 90% of the descending stairs cycle (Fig. 7 (b)). A smaller external rotation (−8.0°) and larger internal rotation (2.2°) were observed in the MPKP (Fig. 7 (c)) compared with those of

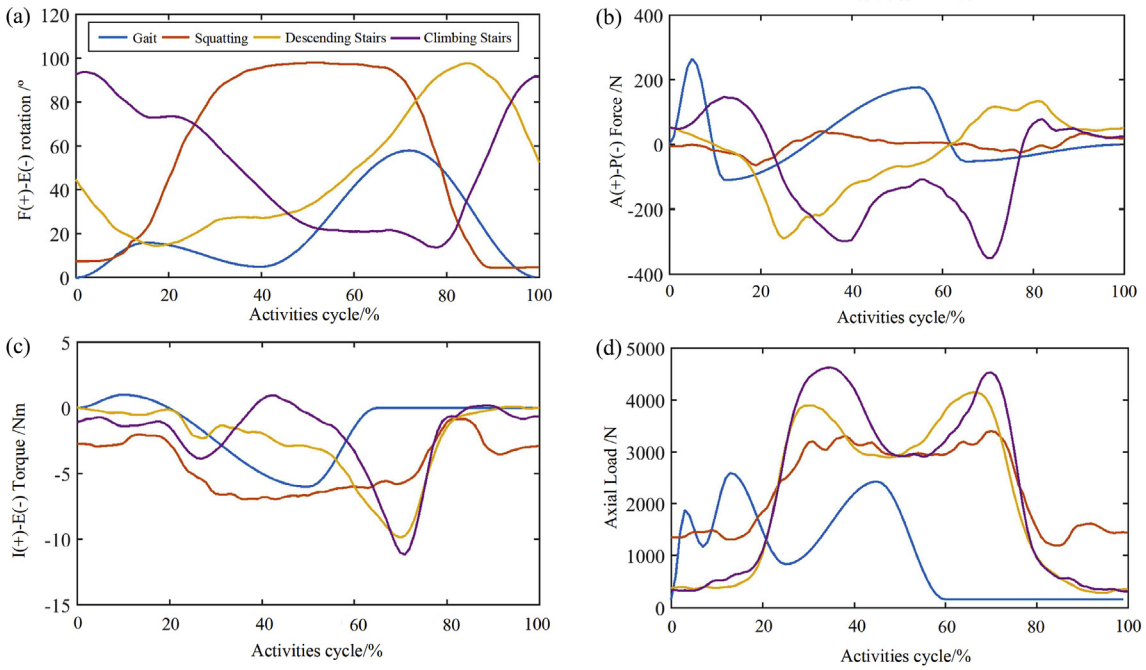

Fig. 3. Boundary conditions of the gait cycle, squatting, descending stairs and climbing stairs. (Note: the boundary conditions of the gait cycle were obtained from ISO 14,243–1:2009; and the boundary conditions of the squatting, descending stairs and climbing stairs were obtained from Bergmann et al. [39]).

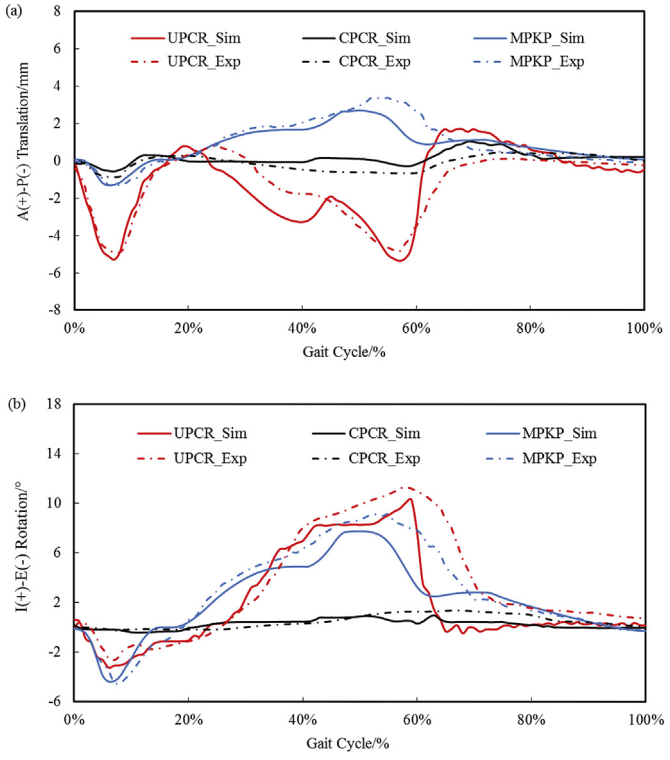

Fig. 4. Model validation of the UPCR, CPCR, and MPKP during the gait cycle. Comparisons of the (a) A–P translation and (b) I–E translation of the TP load point.

the UPCR.

During the climbing stairs cycle, a kinematic performance similar to that of the descending stairs cycle was observed in the three prostheses, as shown in Fig. 8. However, the femoral medial condyle of the MPKP was internally rotated and then externally rotated with no translation. The maximum internal rotation and external rotation were 3.6° and −9.2°, respectively.

3.3. Contact mechanics difference

Fig. 9 shows a comparison of the peak contact pressures on the lateral and medial sides of the three prostheses during daily activities. A higher contact pressure was observed on the UPCR compared with that on the CPCR and MPKP for all of the daily activities. The peak contact pressure on the medial side of the UPCR was higher than that on the lateral side, while the peak contact pressure on the lateral side of the MPKP was higher than that on the medial side. For the CPCR case, the peak contact pressure on the medial and lateral sides exhibited a similar magnitude and trend. The peak contact pressure on the medial side of the MPKP had a magnitude and trend similar to that of the CPCR, while on the lateral side, it was similar to that of the UPCR. However, the peak contact pressure on the medial side of the MPKP was higher than that on the lateral side during 40%–60% of the squatting cycle, owing to the reduced contact area at the large flexion angle (> 90°). Comparisons of the three prostheses for the contact pressure contour generated at the peak axial load during the daily activities are shown in Fig. 10.

4. Discussion

The differences between the joint kinematics and contact mechanics among different intercondylar sagittal conformity implant designs during daily activities were analyzed in this study using an explicit FEM. The accuracy of the simulator was verified using experimental results on gait cycle. The change of the intercondylar sagittal conformity resulted in a decreased the contact pressure, at also changed the kinematics of the femoral component.

In this study, the MPKP demonstrated medial pivot kinematics during the simulated daily activities, which agreed well with previous *in vivo* and *in vitro* clinical results in terms of the trend and magnitude. For example, Schmidt et al. [45] showed that a medial pivot motion with femoral internal (1.4°) and external rotations (−1.9°) was observed during the stance and swing phases of the gait cycle, respectively, through a fluoroscopic analysis of five patients using the MPKP.

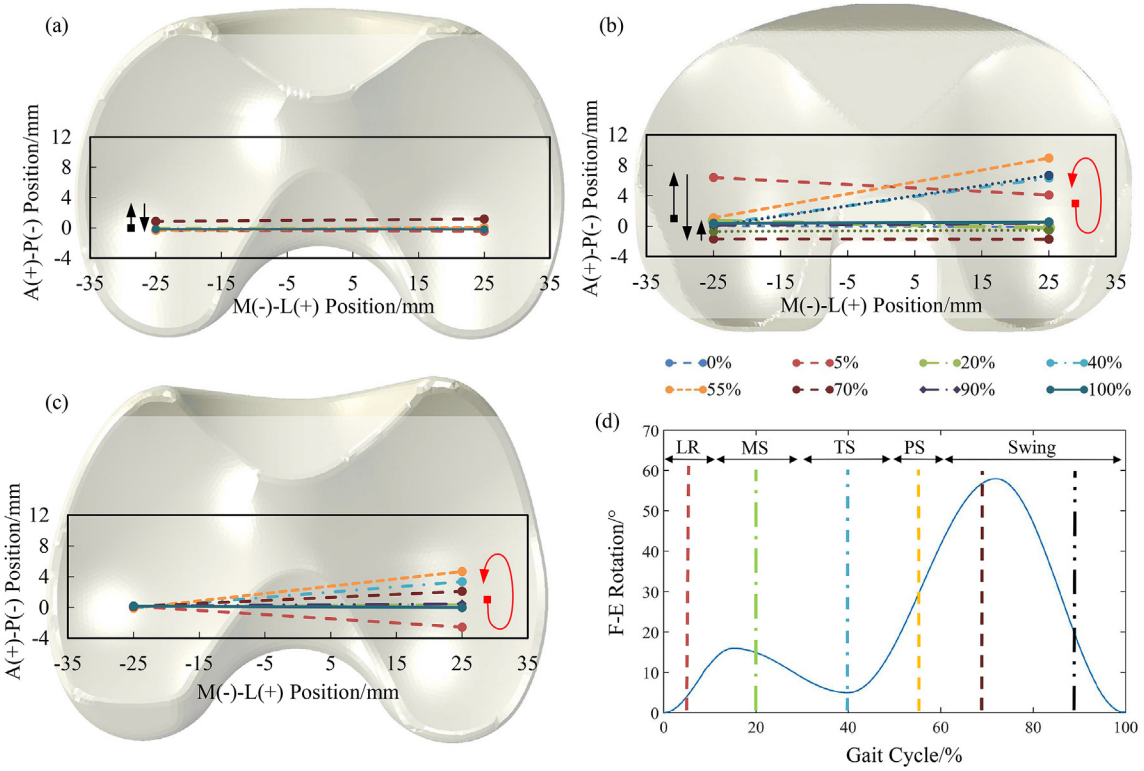

Fig. 5. Comparison of the movement of the femoral flexion axis of the three prostheses during the gait cycle. Femur kinematics of the (a) CPCR, (b) UPCR, and (c) MPKP. (d) F–E angle of the gait cycle (LR: loading response, MS: mid stance, TS: terminal stance, and PS: pre-swing).

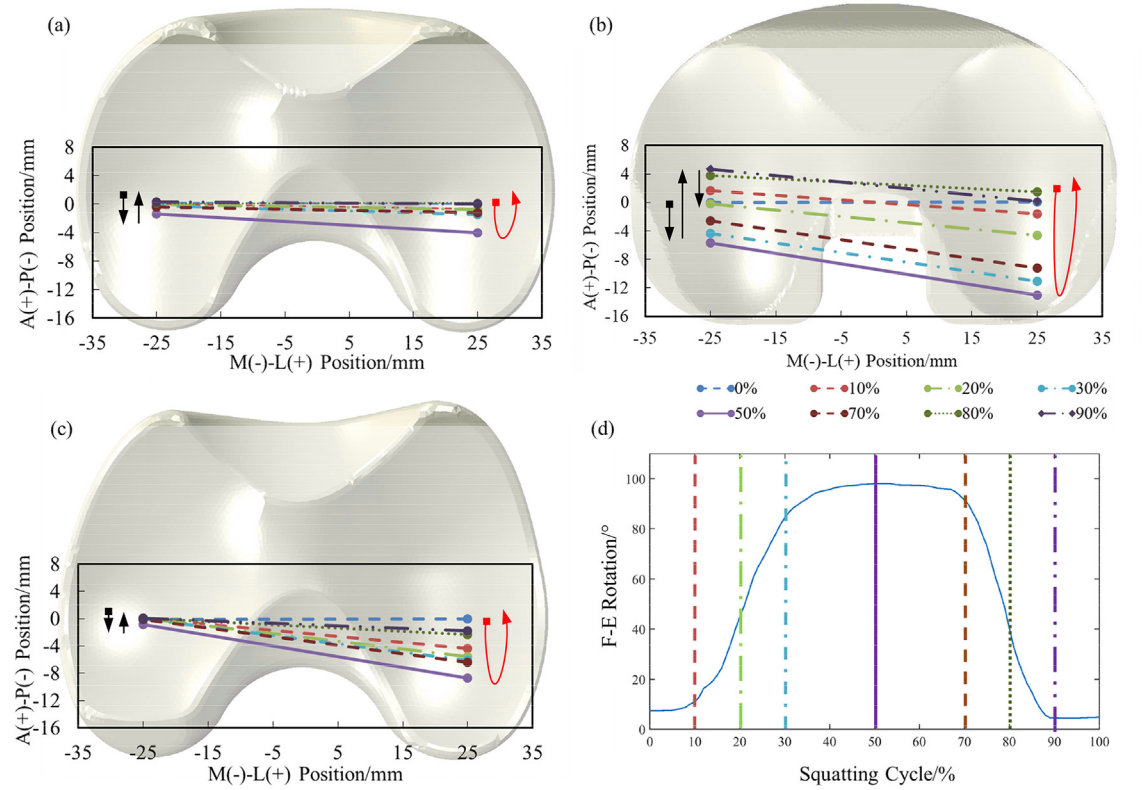

Fig. 6. Comparison of the movement of the femoral flexion axis of the three prostheses during the squatting cycle. Femur kinematics of the (a) CPCR, (b) UPCR, and (c) MPKP. (d) F–E angle of the squatting cycle.

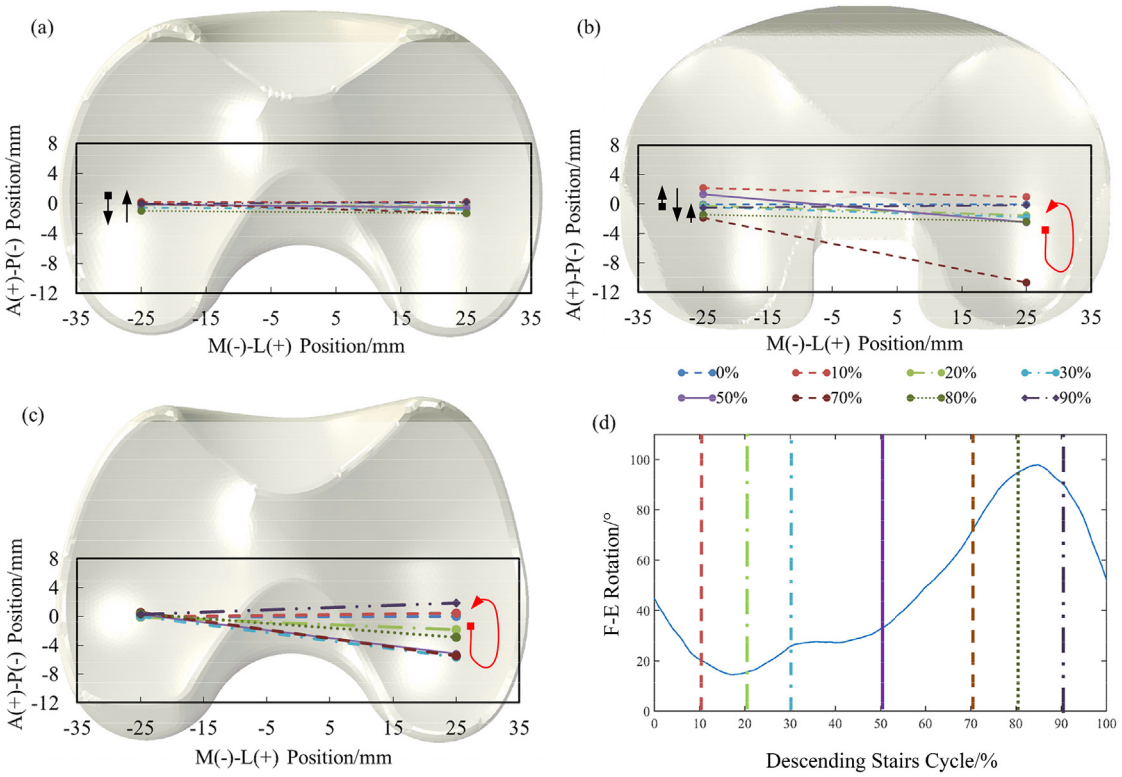

Fig. 7. Comparison of the movement of the femoral flexion axis of the three prostheses during the descending stairs cycle. Femur kinematics of the (a) CPCR, (b) UPCR, and (c) MPKP. (d) F–E angle of the descending stairs cycle.

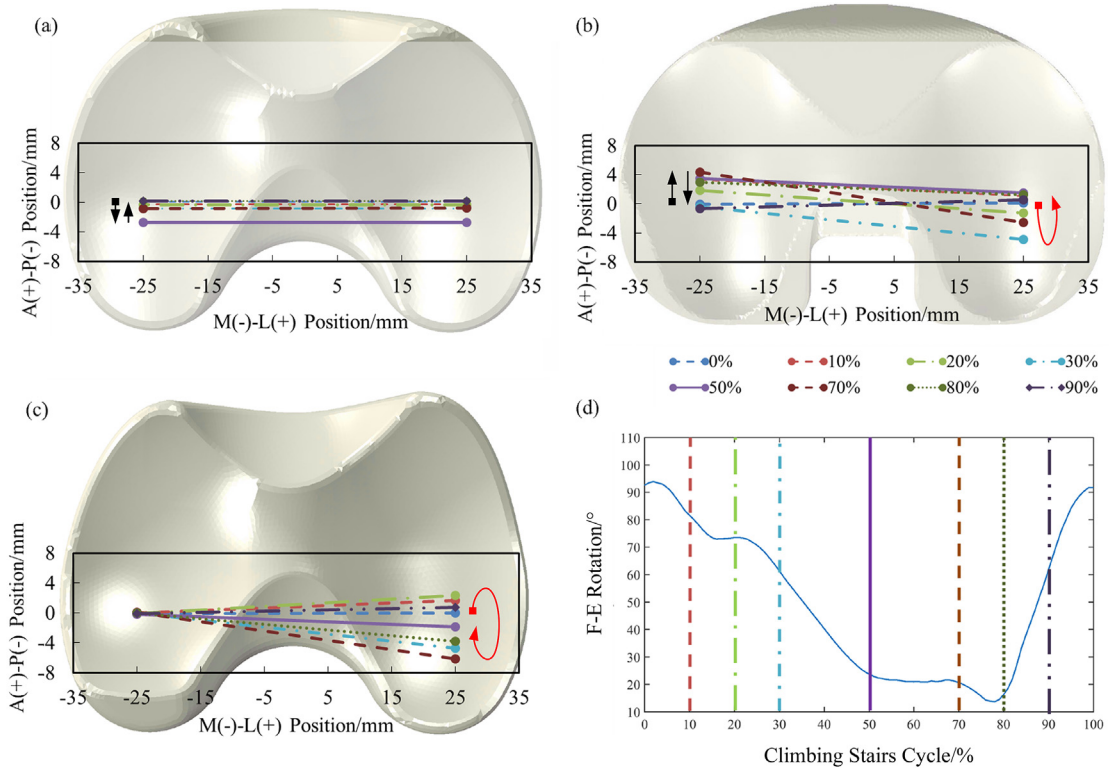

Fig. 8. Comparison of the movement of the femoral flexion axis of the three prostheses during the climbing stairs cycle. Femur kinematics of the (a) CPCR, (b) UPCR, and (c) MPKP. (d) F–E angle of the climbing stairs cycle.

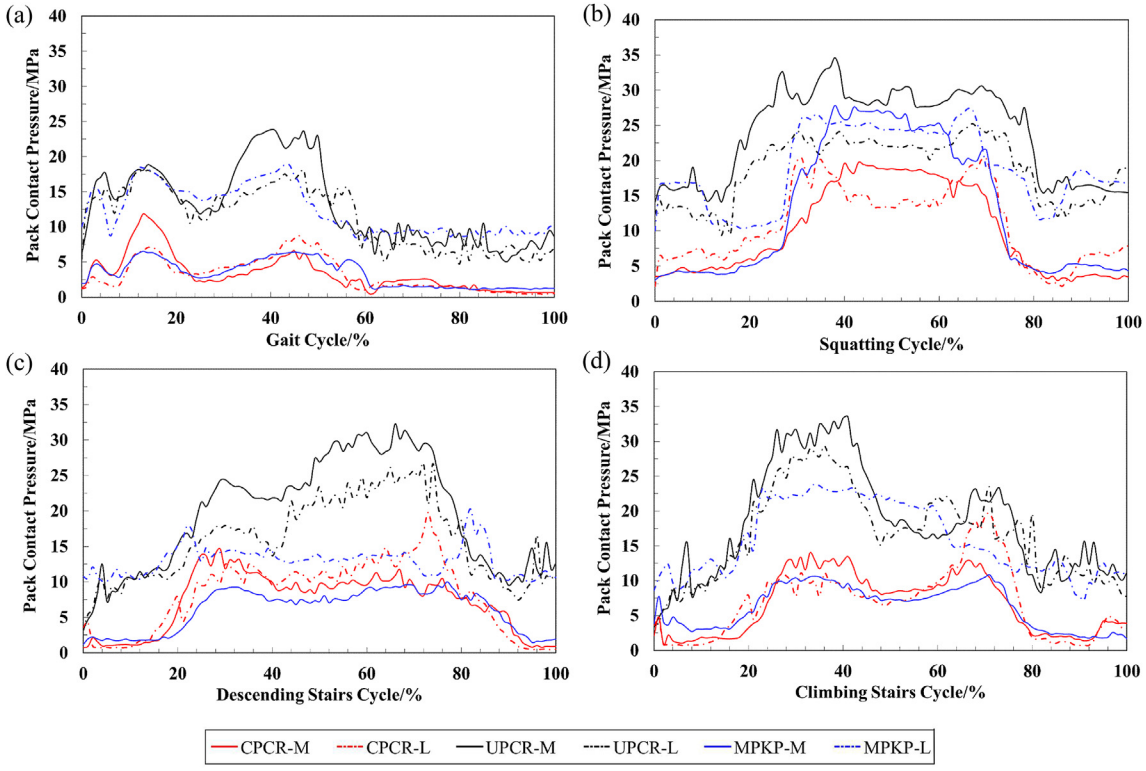

Fig. 9. Comparison of the peak contact pressure for the three prostheses during the (a) gait, (b) squatting, (c) descending stairs, and (d) climbing stairs cycles.

Moonot et al. [24] demonstrated medial pivot motion with femoral external rotation ($-5 \pm 3°$) during squatting. Scott et al. [46] reported a similar motion with femoral internal and external rotations during climbing and descending stairs activities. The medial pivot motion of the MPKP is consistent with the kinematics of a healthy knee joint, which may increase patient satisfaction [47]. However, the I-E rotation pattern of the MPKP knee showed slight differences with the averaged motion of a healthy knee, small internal rotations were observed during the stance phase of the gait (3.9°), descending stairs (2.2°), and climbing stairs (3.6°) cycles. The femoral internal rotation may cause a

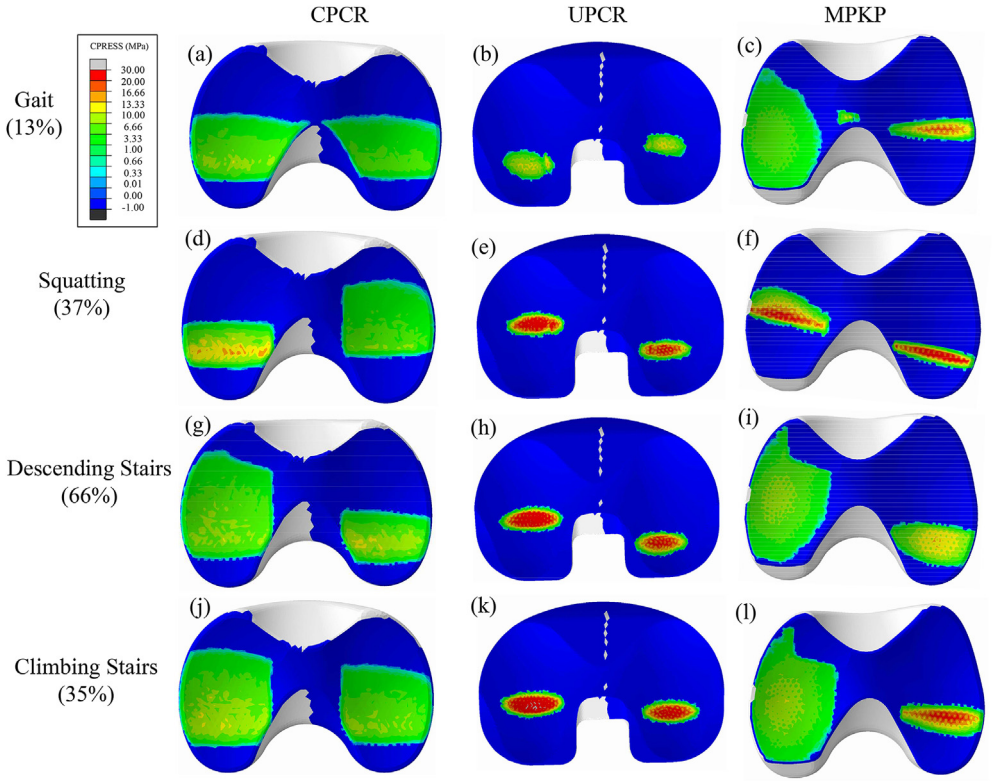

Fig. 10. Contact pressure contour map of the three prostheses generated at the peak axial load during the daily activities.

higher forced lateral A–P translation, which would result in greater tension on the anterolateral soft tissues and pain in this area. This pain has been reported in clinical studies [48,49].

For the CR prosthesis case, the UPCR exhibited a larger parallel posterior translation of the femoral condyles than those on the CPCR and MPKP in the aforementioned four activities. This may increase the risk of wear [50,51]. The *in vivo* studies performed by Nishio et al. [52] were comparable to the predicted results of this study, which showed a medial translation of 7 mm in the squatting cycle for 10°–120° of flexion. In addition, a paradoxical anterior translation was observed during the stance phase of the gait, descending stairs, and climbing stairs cycles, which is consistent with *in-vivo* fluoroscopic measurements [53–56]. Varadarajan et al. [25] also observed a 5.2 mm anterior translation during the climbing stairs cycle on the medial side of the Vanguard-CR design (Biomet Inc., Warsaw, IN) through computational simulation. This design is similar to the UPCR. However, a few studies have presented controversial results regarding the clinical outcome of the UPCR design [57,58]. For example, Horiuchi et al. [57], presented medial pivot behavior that was also found in NRG CR cementless knee prostheses during weight-bearing deep squatting. The sagittal design is similar to that of the UPCR. This controversial result may be mainly caused by the special spherical arc design in the transverse plane, which could guide the motion of the femoral component. The CPCR was prone to a hinge-joint kinematic performance in all activities. These kinematic alterations of the CR designs were mainly related to their symmetrical articular geometries, compared with the healthy knee.

It is known that the sagittal conformity has a direct influence on contact stress. The contact pressure on the medial and lateral sides of the three prostheses were compared separately in this study because of their different sagittal conformities. For the medial compartment case, a smaller contact pressure and larger contact area were observed on the MPKP and CPCR compared with those of the UPCR owing to the higher sagittal conformity, as shown in Figs. 9 and 10. A lower pressure combined with a small slide distance decreases the wear of a TP component [21,59–61]. For the lateral side case, the contact pressure on the MPKP was greater than that on the CPCR for all activities, and occasionally greater than that on the UPCR. Thus, there was a risk of wear on the lateral side of the MPKP. Steinbrück et al. [62] also reported a similar experimental result during squatting. However, the total amount of wear on the MPKP and CPCR was less than that on the UPCR owing to the small contact pressure on the medial side according to the Archard's wear law [50]. Minoda et al. [63] analyzed the synovial fluid of patients after accepting the MPKP and a posterior-stabilized prosthesis. The total number of particles on the MPKP knee was less than half of that in the knee with a posterior-stabilized prosthesis. However, a long-term study comprising a wear comparison of the CR designs and MPKP has not been performed. As the wear on the unilateral side of the prosthesis would impact the service life, it is still difficult to determine which design has a longer service life owing to the high pressure and large slide distance on the lateral side of the MPKP.

The maximum contact pressure can be used to estimate the potential and localized damage to the TP component. The maximum contact pressure was compared in the three prostheses for the four activities, as shown in Fig. 11. The UPCR exhibited the highest maximum contact pressure, which exceeds the yield stress (24.79 MPa) of the UHMWP. In addition, the highest pressure on the prosthesis was produced occurred squatting despite the low axial force generated during the squatting cycle. Therefore, squatting could damage the TP component. Similar results were also found in previous studies [64].

There were limitations and assumptions associated with this study. An ideal alignment and position of the prosthesis components was assumed during simulation. Small malalignments with postoperative coronal, sagittal, and rotational alignment that were found in actual TKA surgeries were ignored [65–67]. For the TKR model, mobile bearing CPCR and MPKP models were used instead of fixed models due to the access difficulty to the 3D CAD model. The influence of the difference between the fixed and mobile TKA designs on the simulation results should be further analyzed. However, most commercial designs do not change the femorotibial interface design of the TP component, and only add the hinge joint between the TP and tibial tray components, compared with the fixed and mobile bearing TKR designs. Moreover, the multi-radius design of the UPCR also influences the kinematics and contact mechanics of the implant performance, which might limits the simulation results used directly in the design analysis. For the simulator, the muscle force and interaction between femur and patella were not considered in the model, which might influence the kinematics and contact mechanics of the prosthesis [68–70]. A higher fidelity knee simulator including the patellofemoral joint and muscle loading should be implemented to analyze the comprehensive characteristics of TKA knee joints. Furthermore, the boundary conditions were fixed for all of the designs, however, the implant geometry and subject-specific differences would cause a change in the loading condition on the prostheses. The predicted change remains a challenge, which should be considered in future studies.

5. Conclusions

The differences in the kinematics and contact mechanics of symmetrical CR, and MPKP designs were investigated for daily activities using an explicit FEM. The predicted kinematic results demonstrated that the MPKP had similar kinematics as healthy knee, with no paradoxical motion of the femur that was observed for the UPCR. However, a small femoral internal rotation was observed during the gait, descending stairs, and climbing stairs cycles. This may result in anterolateral pain for the MPKP knee. For the contact pressure distribution case, the magnitude of the peak contact pressure on the medial side of

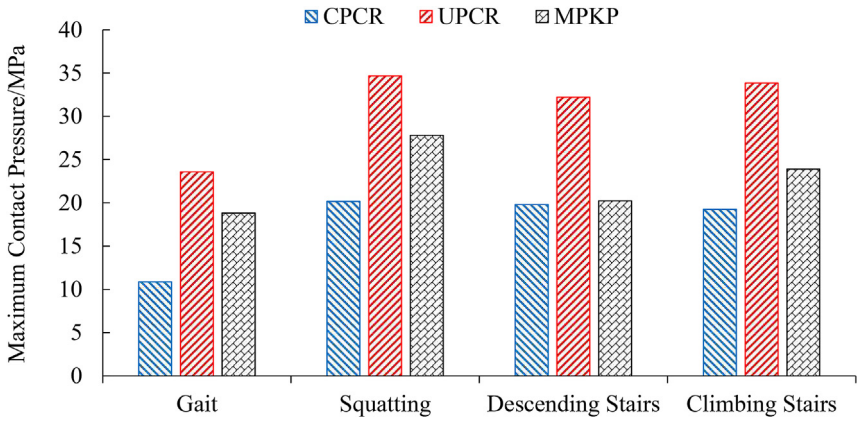

Fig. 11. Comparison of the maximum contact pressure of the three prostheses during daily activities.

the MPKP was obviously reduced, while the lateral side exhibited no significant difference compared to that of the UPCR. Thus, further *in vivo* analysis and long-term studies on the wear comparison of the CR designs and MPKP are required.

Acknowledgements

We thank Prof. Georg Bergmann and his colleagues as the organizers of the Orthoload database for making the invaluable *in vivo* experimental data publicly available. This research was supported by JSPS KAKENHI Grant Number 16H05874.

References

[1] B.C. Carr, T. Goswami, Knee implants - review of models and biomechanics, Mater. Des. 30 (2009) 398–413, https://doi.org/10.1016/j.matdes.2008.03.032.
[2] J. de Beer, D. Petruccelli, A. Adili, L. Piccirillo, D. Wismer, M. Winemaker, Patient perspective survey of total hip vs total knee arthroplasty surgery, J. Arthroplast. 27 (2012) 865–869, https://doi.org/10.1016/j.arth.2011.12.031 e5.
[3] J.D. Blaha, The rationale for a total knee implant that confers anteroposterior stability throughout range of motion, J. Arthroplast. 19 (2004) 22–26, https://doi.org/10.1016/j.arth.2004.04.002.
[4] J. Stiehl, R. Komistek, D. Dennis, R. Paxson, W. Hoff, Fluoroscopic analysis of kinematics after posterior-cruciate-retaining knee arthroplasty, J. Bone Joint Surg. Br. 77–B (1995) 884–889, https://doi.org/10.1302/0301-620X.77B6.7593100.
[5] F. Ansari, M.D. Ries, L. Pruitt, Effect of processing, sterilization and crosslinking on UHMWPE fatigue fracture and fatigue wear mechanisms in joint arthroplasty, J. Mech. Behav. Biomed. Mater. 53 (2016) 329–340, https://doi.org/10.1016/j.jmbbm.2015.08.026.
[6] A.H. Alzamora, J.I.M. Arza, J.U. Zarranz, F.D. Renovales, Anthropometry of the cruciate ligaments of the knee : MRI study of the human four-bar linkage device, Eur. J. Anat. 21 (2017) 1–11.
[7] Y. Feng, T.Y. Tsai, J.S. Li, H.E. Rubash, G. Li, A. Freiberg, In-vivo analysis of flexion axes of the knee: femoral condylar motion during dynamic knee flexion, Clin. Biomech. 32 (2016) 102–107, https://doi.org/10.1016/j.clinbiomech.2015.12.006.
[8] D.A. Dennis, M.R. Mahfouz, R.D. Komistek, W. Hoff, In vivo determination of normal and anterior cruciate ligament-deficient knee kinematics, J. Biomech. 38 (2005) 241–253, https://doi.org/10.1016/j.jbiomech.2004.02.042.
[9] F. Leszko, K.R. Hovinga, A.L. Lerner, R.D. Komistek, M.R. Mahfouz, In vivo normal knee kinematics: is ethnicity or gender an influencing factor? Clin. Orthop. Relat. Res. 469 (2011) 95–106, https://doi.org/10.1007/s11999-010-1517-z.
[10] O. Tanifuji, T. Sato, K. Kobayashi, T. Mochizuki, Y. Koga, H. Yamagiwa, G. Omori, N. Endo, Three-dimensional in vivo motion analysis of normal knees employing transepicondylar axis as an evaluation parameter, Knee Surgery, Sport, Traumatol. Arthrosc. 21 (2013) 2301–2308, https://doi.org/10.1007/s00167-012-2010-x.
[11] T.A. Moro-Oka, S. Hamai, H. Miura, T. Shimoto, H. Higaki, B.J. Fregly, Y. Iwamoto, S.A. Banks, Dynamic activity dependence of in vivo normal knee kinematics, J. Orthop. Res. 26 (2008) 428–434, https://doi.org/10.1002/jor.20488.
[12] T. Karachalios, S. Varitimidis, K. Bargiotas, M. Hantes, N. Roidis, K.N. Malizos, An 11- to 15-year clinical outcome study of the Advance Medial Pivot total knee arthroplasty: pivot knee arthroplasty, Bone Jt. J. 98–B (2016) 1050–1055, https://doi.org/10.1302/0301620X.98B8.36208.
[13] L. Sabatini, S. Risitano, G. Parisi, F. Tosto, P.F. Indelli, F. Atzori, A. Massè, Medial pivot in total knee arthroplasty: literature review and our first experience, Clin. Med. Insights Arthritis Musculoskelet. Disord. 11 (2018) 0–3, https://doi.org/10.1177/1179544117751431.
[14] A. Shimmin, S. Martinez-Martos, J. Owens, A.D. Iorgulescu, S. Banks, Fluoroscopic motion study confirming the stability of a medial pivot design total knee arthroplasty, Knee 22 (2015) 522–526, https://doi.org/10.1016/j.knee.2014.11.011.
[15] G. Castellarin, S. Pianigiani, B. Innocenti, Asymmetric polyethylene inserts promote favorable kinematics and better clinical outcome compared to symmetric inserts in a mobile bearing total knee arthroplasty, Knee Surgery, Sport, Traumatol. Arthrosc. 0 (2018), https://doi.org/10.1007/s00167-018-5207-9.
[16] C.Y. Fan, J.T.S. Hsieh, M.S. Hsieh, Y.C. Shih, C.H. Lee, Primitive results after medial-pivot knee arthroplasties. A minimum 5-year follow-up study, J. Arthroplast. 25 (2010) 492–496, https://doi.org/10.1016/j.arth.2009.05.008.
[17] T. Karachalios, N. Roidis, D. Giotikas, K. Bargiotas, S. Varitimidis, K.N. Malizos, A mid-term clinical outcome study of the Advance Medial Pivot knee arthroplasty, Knee 16 (2009) 484–488, https://doi.org/10.1016/j.knee.2009.03.002.
[18] Y.H. Kim, S.H. Yoon, J.S. Kim, Early outcome of TKA with a medial pivot fixed-bearing prosthesis is worse than with a PFC mobile-bearing prosthesis, Clin. Orthop. Relat. Res. 467 (2009) 493–503, https://doi.org/10.1007/s11999-008-0221-8.
[19] Y.-H. Kim, J.-W. Park, J.-S. Kim, Clinical outcome of medial pivot compared with press-fit condylar sigma cruciate-retaining mobile-bearing total knee arthroplasty, J. Arthroplast. 32 (2017) 3016–3023, https://doi.org/10.1016/j.arth.2017.05.022.
[20] G.I. Papagiannis, I.M. Roumpelakis, A.I. Triantafyllou, I.N. Makris, G.C. Babis, No differences identified in transverse plane biomechanics between medial pivot and rotating platform total knee implant designs, J. Arthroplast. 31 (2016) 1814–1820, https://doi.org/10.1016/j.arth.2016.01.050.
[21] B.J. Fregly, W.G. Sawyer, M.K. Harman, S.A. Banks, Computational wear prediction of a total knee replacement from in vivo kinematics, J. Biomech. 38 (2005) 305–314, https://doi.org/10.1016/j.jbiomech.2004.02.013.
[22] L.A. Knight, S. Pal, J.C. Coleman, F. Bronson, H. Haider, D.L. Levine, M. Taylor, P.J. Rullkoetter, Comparison of long-term numerical and experimental total knee replacement wear during simulated gait loading, J. Biomech. 40 (2007) 1550–1558, https://doi.org/10.1016/j.jbiomech.2006.07.027.
[23] S. O'Brien, Y. Luo, C. Wu, M. Petrak, E. Bohm, J.M. Brandt, Computational development of a polyethylene wear model for the articular and backside surfaces in modular total knee replacements, Tribol. Int. 59 (2013) 284–291, https://doi.org/10.1016/j.triboint.2012.03.020.
[24] P. Moonot, S. Mu, G.T. Railton, R.E. Field, S.A. Banks, Tibiofemoral kinematic analysis of knee flexion for a medial pivot knee, Knee Surgery, Sport, Traumatol. Arthrosc. 17 (2009) 927–934, https://doi.org/10.1007/s00167-009-0777-1.
[25] K.M.M. Varadarajan, T. Zumbrunn, H.E. Rubash, H. Malchau, G. Li, O.K. Muratoglu, Cruciate retaining implant with biomimetic articular surface to reproduce activity dependent kinematics of the normal knee, J. Arthroplast. 30 (2015) 2149–2153, https://doi.org/10.1016/j.arth.2015.06.018 e2.
[26] A.C. Godest, M. Beaugonin, E. Haug, M. Taylor, P.J. Gregson, Simulation of a knee joint replacement during a gait cycle using explicit finite element analysis, J. Biomech. 35 (2002) 267–275, https://doi.org/10.1016/S0021-9290(01)00179-8.
[27] J.P. Halloran, A.J. Petrella, P.J. Rullkoetter, Explicit finite element modeling of total knee replacement mechanics, J. Biomech. 38 (2005) 323–331, https://doi.org/10.1016/j.jbiomech.2004.02.046.
[28] K.T. Kang, J.H. Park, K. Il Lee, Y.B. Shim, J.W. Jang, H.J. Chun, Gait cycle comparions of cruciate sacrifice for total knee design.-explicit finite element, Int. J. Precis. Eng. Manuf. 13 (2012) 2043–2049, https://doi.org/10.1007/s12541-012-0269-y.
[29] A.R. Hopkins, A.M. New, F. Rodriguez-y-Baena, M. Taylor, Finite element analysis of unicompartmental knee arthroplasty, Med. Eng. Phys. 32 (2010) 14–21, https://doi.org/10.1016/j.medengphy.2009.10.002.
[30] L. Shu, K. Yamamoto, J. Yao, P. Saraswat, Y. Liu, M. Mitsuishi, N. Sugita, A subject-specific finite element musculoskeletal framework for mechanics analysis of a total knee replacement, J. Biomech. 77 (2018) 146–154, https://doi.org/10.1016/j.jbiomech.2018.07.008.
[31] P.S. Walker, G.W. Blunn, D.R. Broome, J. Perry, A. Watkins, S. Sathasivam, M.E. Dewar, J.P. Paul, A knee simulating machine for performance evaluation of total knee replacements, J. Biomech. 30 (1997) 83–89, https://doi.org/10.1016/S0021-9290(96)00118-2.
[32] D. Zhao, H. Sakoda, W.G. Sawyer, S.A. Banks, B.J. Fregly, Predicting knee replacement damage in a simulator machine using a computational model with a consistent wear factor, J. Biomech. Eng. 130 (2008) 11004, https://doi.org/10.1115/1.2838030.
[33] A. Abdelgaied, F. Liu, C. Brockett, L. Jennings, J. Fisher, Z. Jin, Computational wear prediction of artificial knee joints based on a new wear law and formulation, J. Biomech. 44 (2011) 1108–1116, https://doi.org/10.1016/j.jbiomech.2011.01.027.
[34] J. Zhang, Z. Chen, L. Wang, D. Li, Z. Jin, A patient-specific wear prediction framework for an artificial knee joint with coupled musculoskeletal multibody-dynamics and finite element analysis, Tribol. Int. 109 (2017) 382–389, https://doi.org/10.1016/j.triboint.2016.10.050.
[35] M.M. Ardestani, M. Moazen, E. Maniei, Z. Jin, Posterior stabilized versus cruciate retaining total knee arthroplasty designs: conformity affects the performance reliability of the design over the patient population, Med. Eng. Phys. 37 (2015) 350–360, https://doi.org/10.1016/j.medengphy.2015.01.008.
[36] C.K. Fitzpatrick, C. Maag, C.W. Clary, A. Metcalfe, J. Langhorn, P.J. Rullkoetter, Validation of a new computational 6-DOF knee simulator during dynamic activities, J. Biomech. 49 (2016) 3177–3184, https://doi.org/10.1016/j.jbiomech.2016.07.040.
[37] S.M. Kurtz, UHMWPE Biomaterials Handbook, Elsevier, 2016, https://doi.org/10.1016/C2013-0-16083-7.
[38] T. Fukubayashi, P.A. Torzilli, M.F. Sherman, R.F. Warren, An in vitro biomechanical evaluation of anterior-posterior motion of the knee. Tibial displacement, rotation, and torque, J. Bone Jt. Surg. 64 (1982) 258–264.
[39] G. Bergmann, A. Bender, F. Graichen, J. Dymke, A. Rohlmann, A. Trepczynski, M.O. Heller, I. Kutzner, Standardized loads acting in knee implants, PLoS One 9 (2014) e86035, , https://doi.org/10.1371/journal.pone.0086035.
[40] W.R. Taylor, E.I. Kornaropoulos, G.N. Duda, S. Kratzenstein, R.M. Ehrig, A. Arampatzis, M.O. Heller, Repeatability and reproducibility of OSSCA, a functional approach for assessing the kinematics of the lower limb, Gait Posture 32 (2010) 231–236, https://doi.org/10.1016/j.gaitpost.2010.05.005.
[41] A. Trepczynski, I. Kutzner, E. Kornaropoulos, W.R. Taylor, G.N. Duda, G. Bergmann, M.O. Heller, Patellofemoral joint contact forces during activities with high knee flexion, J. Orthop. Res. (2012) 408–415, https://doi.org/10.1002/jor.21540.
[42] P. Eichelberger, M. Ferraro, U. Minder, T. Denton, A. Blasimann, F. Krause, H. Baur, Analysis of accuracy in optical motion capture – a protocol for laboratory setup evaluation, J. Biomech. 49 (2016) 2085–2088, https://doi.org/10.1016/j.jbiomech.2016.05.007.
[43] J.D. Desjardins, P.S. Walker, H. Haider, J. Perry, The use of a force-controlled dynamic knee simulator to quantify the mechanical performance of total knee replacement designs during functional activity, J. Biomech. 33 (2000) 1231–1242, https://doi.org/10.1016/S0021-9290(00)00094-4.
[44] J.P. Halloran, S.K. Easley, A.J. Petrella, P.J. Rullkoetter, Comparison of deformable and elastic foundation finite element simulations for predicting knee replacement mechanics, J. Biomech. Eng. 127 (2005) 813–818, https://doi.org/10.1115/1.1992522.
[45] R. Schmidt, R.D. Komistek, J.D. Blaha, B.L. Penenberg, W.J. Maloney, Fluoroscopic analyses of cruciate-retaining and medial pivot knee implants, Clin. Orthop. Relat. Res. 410 (2003) 139–147, https://doi.org/10.1097/01.blo.0000063565.90853.a4.

[46] G. Scott, M.A. Imam, A. Eifert, Freeman, V. Pinskerova, R.E. Field, J. Skinner, S. Banks, Can a total knee arthroplasty be both rotationally unconstrained and anteroposteriorly stabilised? Bone Jt. Res. 5 (2016) 80–86, https://doi.org/10.1302/2046-3758.53.2000621.

[47] R.D. Komistek, D. a Dennis, M. Mahfouz, In vivo fluoroscopic analysis of the normal human knee, Clin. Orthop. Relat. Res. (2003) 69–81, https://doi.org/10.1097/01.blo.0000062384.79828.3b.

[48] C. Halewood, M. Risebury, N.P. Thomas, A.A. Amis, Kinematic behaviour and soft tissue management in guided motion total knee replacement, Knee Surgery, Sport, Traumatol. Arthrosc. 22 (2014) 3074–3082, https://doi.org/10.1007/s00167-014-2933-5.

[49] L. Luyckx, T. Luyckx, J. Bellemans, J. Victor, Iliotibial band traction syndrome in guided motion TKA. A new clinical entity after TKA, Acta Orthop. Belg. 76 (2010) 507–512 http://www.ncbi.nlm.nih.gov/pubmed/20973358.

[50] J.F. Archard, W. Hirst, The wear of metals under unlubricated conditions, Proc. R. Soc. A Math. Phys. Eng. Sci. 236 (1956) 397–410, https://doi.org/10.1098/rspa.1956.0144.

[51] A. Abdelgaied, J. Fisher, L.M. Jennings, A comprehensive combined experimental and computational framework for pre-clinical wear simulation of total knee replacements, J. Mech. Behav. Biomed. Mater. 78 (2018) 282–291, https://doi.org/10.1016/j.jmbbm.2017.11.022.

[52] Y. Nishio, T. Onodera, Y. Kasahara, D. Takahashi, N. Iwasaki, T. Majima, Intraoperative medial pivot affects deep knee flexion angle and patient-reported outcomes after total knee arthroplasty, J. Arthroplast. 29 (2014) 702–706, https://doi.org/10.1016/j.arth.2013.06.035.

[53] I.M. Zeller, A. Sharma, W.B. Kurtz, M.R. Anderle, R.D. Komistek, Customized versus patient-sized cruciate-retaining total knee arthroplasty: an in vivo kinematics study using mobile fluoroscopy, J. Arthroplast. 32 (2017) 1344–1350, https://doi.org/10.1016/j.arth.2016.09.034.

[54] H.E. Cates, R.D. Komistek, M.R. Mahfouz, M.A. Schmidt, M. Anderle, In vivo comparison of knee kinematics for subjects having either a posterior stabilized or cruciate retaining high-flexion total knee arthroplasty, J. Arthroplast. 23 (2008) 1057–1067, https://doi.org/10.1016/j.arth.2007.09.019.

[55] J. Victor, S. Banks, J. Bellemans, Kinematics of posterior cruciate ligament-retaining and -substituting total knee arthroplasty, J. Bone Joint Surg. Br. 87–B (2005) 646–655, https://doi.org/10.1302/0301-620x.87b5.15602.

[56] T.F. Grieco, A. Sharma, R.D. Komistek, H.E. Cates, Single versus multiple-radii cruciate-retaining total knee arthroplasty: an in vivo mobile fluoroscopy study, J. Arthroplast. 31 (2016) 694–701, https://doi.org/10.1016/j.arth.2015.10.029.

[57] H. Horiuchi, S. Akizuki, T. Tomita, K. Sugamoto, T. Yamazaki, N. Shimizu, In vivo kinematic analysis of cruciate-retaining total knee arthroplasty during weight-bearing and non-weight-bearing deep knee bending, J. Arthroplast. 27 (2012) 1196–1202, https://doi.org/10.1016/j.arth.2012.01.017.

[58] X. Shi, Z. Zhou, B. Shen, J. Yang, P. Kang, F. Pei, Variations in morphological characteristics of prostheses for total knee arthroplasty leading to kinematic differences, Knee 22 (2015) 18–23, https://doi.org/10.1016/j.knee.2014.10.013.

[59] S. Tozzi, E. Modena, S. Falcioni, A. Sudanese, S. Affatato, P. Taddei, The effects of contact area and applied load on the morphology of in vitro worn ultra-high molecular weight knee prostheses: a micro-Raman and gravimetric study, J. Raman Spectrosc. 45 (2014) 781–787, https://doi.org/10.1002/jrs.4545.

[60] J. Reinders, R. Sonntag, J.P. Kretzer, Wear behavior of an unstable knee: stabilization via implant design? BioMed Res. Int. 2014 (2014) 821475, https://doi.org/10.1155/2014/821475.

[61] S. Sathasivam, P.S. Walker, P.A. Campbell, K. Rayner, The effect of contact area on wear in relation to fixed bearing and mobile bearing knee replacements, J. Biomed. Mater. Res. 58 (2001) 282–290, https://doi.org/10.1002/1097-4636(2001)58:3<282::AID-JBM1018>3.0.CO;2-S.

[62] A. Steinbrück, C. Schröder, M. Woiczinski, A. Fottner, V. Pinskerova, P.E. Müller, V. Jansson, Femorotibial kinematics and load patterns after total knee arthroplasty: an in vitro comparison of posterior-stabilized versus medial-stabilized design, Clin. Biomech. 33 (2016) 42–48, https://doi.org/10.1016/j.clinbiomech.2016.02.002.

[63] Y. Minoda, A. Kobayashi, H. Iwaki, K. Iwakiri, F. Inori, R. Sugama, M. Ikebuchi, Y. Kadoya, K. Takaoka, In vivo analysis of polyethylene wear particles after total knee arthroplasty: the influence of improved materials and designs, J. Bone Jt. Surgery-American 91 (2009) 67–73, https://doi.org/10.2106/JBJS.I.00447.

[64] D.D. D'Lima, N. Steklov, B.J. Fregly, S.A. Banks, C.W. Colwell, In vivo contact stresses during activities of daily living after knee arthroplasty, J. Orthop. Res. 26 (2008) 1549–1555, https://doi.org/10.1002/jor.20670.

[65] F.W. Werner, D.C. Ayers, L.P. Maletsky, P.J. Rullkoetter, The effect of valgus/varus malalignment on load distribution in total knee replacements, J. Biomech. 38 (2005) 349–355, https://doi.org/10.1016/j.jbiomech.2004.02.024.

[66] G.S. Dyrhovden, A.M. Fenstad, O. Furnes, Ø. Gøthesen, Survivorship and relative risk of revision in computer-navigated versus conventional total knee replacement at 8-year follow-up, Acta Orthop. 87 (2016) 592–599, https://doi.org/10.1080/17453674.2016.1244884.

[67] Y.H. Kim, J.W. Park, J.S. Kim, S.D. Park, The relationship between the survival of total knee arthroplasty and postoperative coronal, sagittal and rotational alignment of knee prosthesis, Int. Orthop. 38 (2014) 379–385, https://doi.org/10.1007/s00264-013-2097-9.

[68] J. Victor, L. Labey, P. Wong, B. Innocenti, J. Bellemans, The influence of muscle load on tibiofemoral knee kinematics, J. Orthop. Res. 28 (2010) 419–428, https://doi.org/10.1002/jor.21019.

[69] B.A. MacWilliams, D.R. Wilson, J.D. Desjardins, J. Romero, E.Y.S. Chao, Hamstrings cocontraction reduces internal rotation, anterior translation, and anterior cruciate ligament load in weight-bearing flexion, J. Orthop. Res. 17 (1999) 817–822, https://doi.org/10.1002/jor.1100170605.

[70] S.D. Kwak, C.S. Ahmad, T.R. Gardner, R.P. Grelsamer, J.H. Henry, L. Blankevoort, G.A. Ateshian, V.C. Mow, Hamstrings and iliotibial band forces affect knee kinematics and contact pattern, J. Orthop. Res. 18 (2000) 101–108, https://doi.org/10.13832/j.jnpe.2015.S1.0034.